Sorption and desorption of tetrabromobisphenol-A on acidic montmorillonite (K10)

Li Xiang[a,b], Zaili Zhang[a,b], Jia Xiaoshan[a,b,*]

[a]*School of Environmental Science and Engineering, Sun Yat-Sen University, Guangzhou 510275, China, Tel. +86 20 39332690; emails: lix53@mail2.sysu.edu.cn (L. Xiang), eeszzl@mail.sysu.edu.cn (Z. Zhang), eesjxs@126.com (J. Xiaoshan)*
[b]*Guangdong Provincial Key Laboratory of Environmental Pollution Control and Remediation Technology, Guangzhou 510275, China*

ABSTRACT

This work was to examine adsorption of tetrabromobisphenol-A onto acidic montmorillonite (K10) which had been considered as a potential adsorbent for removal of organic pollutants. The Langmuir, Freundlich, Langmuir–Freundlich, and Dubinin–Radushkevich models were applied with determination of sorption and desorption equilibrium isotherms and isotherms constants. The discrimination had been performed by means of various statistics. The results showed that Freundlich and Langmuir–Freundlich models described the sorption isotherms better than Langmuir model. Meanwhile, desorption hysteresis index calculated from Freundlich model was above zero and increased with increasing temperature, indicating occurrence of hysteresis. Preliminary to the isotherms data, adsorption kinetic had been gathered and tested using pseudo-first-order, pseudo-second-order, intra-particle diffusion, and double-exponential models (DEMs). From the kinetic studies, sorption process was completed in 48 h, and followed pseudo-second-order model and DEMs. Cationic surfactant in aqueous solution had positive effect on adsorption process, and the metal cations promoted sorption capacity in the order: $Ni^{2+} > K^+ > Zn^{2+} > Ca^{2+} > Na^+$. The optimum adsorption capacity was provided by the condition of pH 3, $T = 288$ K, and $I = Ni^{2+}$. Additionally, the thermodynamic parameters indicated the sorption was exothermic and spontaneous. The interaction between K10 and TBBPA was investigated using FTIR.

Keywords: K10; Adsorption; Kinetics; Isotherms; FTIR

1. Introduction

During the last decade, the fate and possible effects of TBBPA entering into the environment had gained considerable attention [1–11]. TBBPA had been found in environmental samples, as well as in human plasma, and there was evidence of a possible toxic effect [12–14]. Boecker et al. [15] found that TBBPA was toxic to primary hepatocytes, most likely by destroying mitochondria. TBBPA was also highly immunotoxic in cultures, which was demonstrated by its ability specifically to inhibit the expression of CD25 at concentration as low as 3 μM [16]. Zhang et al. reported that TBBPA exhibited inhibitory effects on T_3-induced expression of TH-response genes and morphological changes in a concentration-dependent manner, with a weak stimulatory action on tadpole development and

*Corresponding author.

TH-response gene expression in the absence of T_3 induction [17,18]. Hence, it was important to develop strategies to decrease and eliminate TBBPA residues in the environment.

Sorption was regarded as a feasible method for the removal of organic contaminants from waters and wastewaters. Adsorption on activated carbons was well-known process for organic contaminants removal. The porous nature of this adsorbent material and its high surface area were favorable properties for adsorption. However, high cost and recovering problems of activated carbon particles from treated water were of disadvantage [19]. Clays such as montmorillonite, sepiolite, and halloysite could be considered as low-cost adsorbents for wastewater treatments. The wide range for application of clays was due to their large surface, high chemical and mechanical stability, and high cation exchange capacity [20]. Recently, acidic montmorillonite (K10) had been characterized for their ability to remove trimethoprim and promethazine hydrochloride and showed that it was a potential and powerful adsorbent [20,21].

In this study, sorption and desorption of TBBPA onto K10 montmorillonite was studied. Equilibrium, kinetics, thermodynamic, and FTIR were used to examine the sorption process. Hysteresis index (HI) was calculated to evaluate desorption process. Meanwhile, the effects of pH, ions strength, and surfactants were also investigated. The objects of this study were to demonstrated potential for removal of TBBPA by K10 montmorillonite and illustrated the mechanism of sorption process.

2. Materials and methods

2.1. Materials

The tetrabromobisphenol A (4,4′-iisopropylidenebis (2, 6-dibromophenol), 99% purity, Mw 543.9 g/mol, CAS number 79-94-7) used in this study was purchased from Sigma Chemical Co., Ltd (USA). The K10 montmorillonite (CAS number 1318-93-0) was obtained from Aladdin Chemistry Co., Ltd (Shanghai, China). Methanol is of high-performance liquid chromatography (HPLC) grade and purchased from Fisher Co., Ltd (ShangHai, China). The ultrapure water was obtained directly from a Nanopure UV deionization system, Barnstead/Thermolyne Co., Ltd (Dubuque, IA, USA). All other chemicals were of analytical grade unless the stated otherwise.

2.2. Batch experiment technique

Batch experiment technique was used to evaluate adsorption characteristics and mechanisms on K10 montmorillonite. Typically, TBBPA was dissolved in methanol as a stock solution (1,000 mg/L) and stored at 4℃. All of the TBBPA experiment samples were prepared to preselected concentration through diluting stock solution by ultrapure water. Methanol concentration was maintained at less 0.3% (v/v) to avoid the co-solvent effects. The tubes were transferred into the incubator and shaken at 150 rpm. After the sorption experiment done, samples were centrifuged at 3,500 rpm for 10 min and supernatants were analyzed by HPLC-UV to determine the residual concentration of TBBPA.

The TBBPA sorption kinetic was performed with initial concentration of 0.55 mg/L. One hundred milligram montmorillonite (K10) was added into a series of tubes containing 20 mL TBBPA solution and strongly shaken in the incubator at 288, 298, and 308 K. During the sorption process, a sample was withdrawn from one tube at a certain time intervals. The contact time was chosen from 1 to 72 h. After centrifugal separation, the amount of TBBPA adsorbed on K10 was calculated by subtracting the final solution concentration of TBBPA as follows:

$$q_e = \frac{(C_0 - C_e)V}{m} \tag{1}$$

where q_e (mg/g) is the amount of TBBPA adsorbed on K10 montmorillonite, C_0 (mg/L) and C_e (mg/L) are the initial and final solution concentration of TBBPA. V (mL) is the volume of solution and m (kg) is the mass of dry adsorbent used.

Desorption was evaluated using decant and refill technique after the completion of sorption experiment [22]. After the 1 mL aliquot was withdrawn, 14 mL of the remaining supernatant was discarded and replaced by 15 mL ultrapure water. After dilution, the container was agitated for the same time as used in sorption experiment. One milliliter of supernatant was collected for analysis. All of the experiments were carried out in duplicate. The overall mass loss was (<5%) in 72 h, then it was ignored.

The effect of pH on TBBPA uptake by K10 was investigated in a pH range from 3 to 9. A series of tubes containing K10 and TBBPA solution with preselected concentrations were shaken at different pH to equilibrium. After centrifugation, the pH value and the residual TBBPA of the supernatants were measured.

The impact of anions was investigated using sodium salts of nitrate (NO_3^-), sulfate (SO_4^{2-}), phosphate (HPO_4^{2-} and PO_4^{3-}), or carbonate (HCO_3^-). The impact of cations was investigated using chloride of sodium (Na^+), potassium (K^+), calcium (Ca^{2+}), zinc (Zn^{2+}), or nickel (Ni^{2+}). The sorption experiment of anions and cations were carried out at three different concentrations. Solutions mixed with TBBPA and three initial concentrations of anions or cations were prepared. The effects of surfactants (Sodium dodecyl sulfate (SDS) and cetyltrimethyl ammonium bromide (CTMAB)) were also conducted as a similar procedure as ions experiment in different concentrations (from 1.47 to 138.9 mg/L) except that surfactants was firstly added into the system for 12 h and then followed by the injection of TBBPA.

2.3. Analytical methods

The content of each sample was determined by HPLC (Shimadzu LC-20AT, Kyoto, Japan) equipped with a UV detector (SPD-M2OAV) and a VP-ODS column (150 mm × 4.6 mm, 5 μm), all of which were supplied by Shimadzu (Kyoto, Japan). The column was operated at 35°C. A mixture of water and methanol (20:80) at a flow rate of 0.8 mL/min was used as a mobile phase in an isocratic elution mode. The injection volume was 20 μL for all the solutions, and the detection was performed at the wavelength of 209 nm. The pH value of supernatants was detected by EL20 pH meter (Mettler Toledo Instruments Co., Ltd (Shanghai, China)). The TBBPA, K10, K10 loaded with TBBPA, K10 loaded with CTMAB and K10 loaded with TBBPA+CTMAB were characterized by Fourier transform infrared (FTIR) Spectra between 4,000 and 400 cm^{-1}.

2.4. Data analysis

In the present work, the discrimination among different models had been performed on the basis of the some classical statistical criteria such as the Student's *t*-test on the estimated parameters, the sum of squared errors (SSE), the multiple correlation coefficient (*R*), and the coefficient of multiple determination (R^2). Further decision tools, namely the prediction error sum (PRESS) [23] and the Akaike information criteria (AIC) [24] had been also used. The model with the lowest PRESS and AIC values had been considered as the more reliable one.

3. Results and discussion

3.1. Effects of contact time and temperature

The sorption behavior of TBBPA on K10 montmorillonite in relation to contact time was investigated at 288, 298, and 308 K. The pH value in this section was in the range of 4.83–4.92. Under these experimental conditions, TBBPA ($pK_a = 7.5$ and 8.5 [8]) existed in neutral formation. The effect of deprotonation of TBBPA could be excluded from consideration. The plots of time *t* vs. amounts of sorption of TBBPA were presented in Fig. 1(a). It was observed that the amounts of neutral molecule of TBBPA adsorbed onto
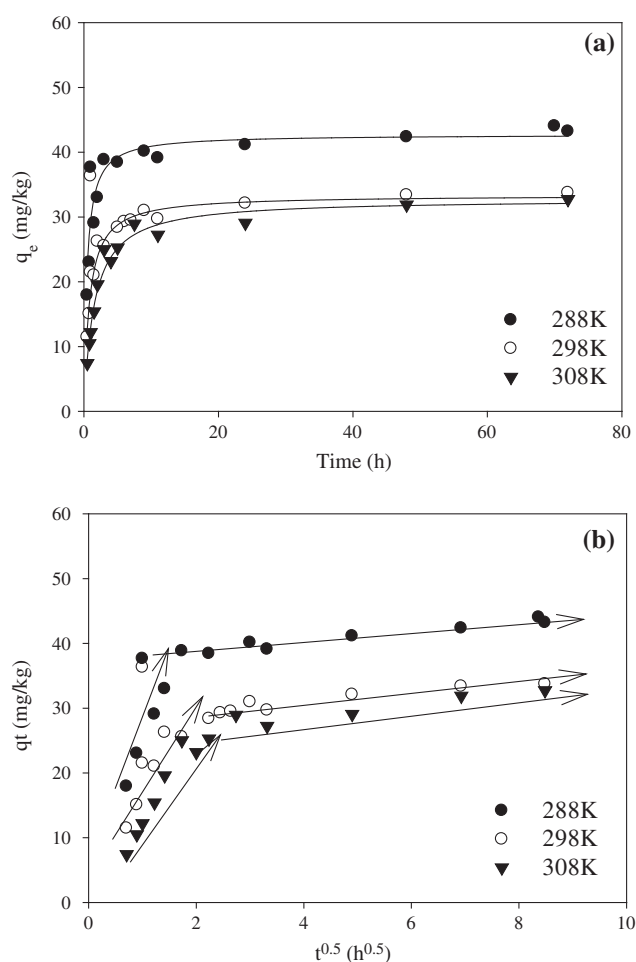
Fig. 1. TBBPA sorption kinetics on K10 (TBBPA-0.55 mg/L; *T*—288, 298, and 308 K; K10—0.1 g; pH 4.83–4.92; (a) effect of contact time, the solid lines are pseudo-second-order simulation and (b) plots of intra-particle diffusion model).

K10 were increased with time increasing, and all of the sorption equilibriums were achieved in 48 h. According to this result, 48 h was selected as the sorption equilibrium time for the batch experiment. The sorption capacities at low initial concentration (0.55 mg/L) were 44.1 mg/kg, 33.7 mg/kg and 32.7 mg/kg for the 288, 298, and 308 K, respectively. Moreover, the sorption capacities were found to decrease when temperature was increased from 288 to 308 K, which implied that adsorption of TBBPA onto K10 was exothermic process. Similar results had been reported for adsorption of TBBPA onto carbon nanotubes and graphene oxide [9,25].

3.2. Sorption kinetics

3.2.1. Pseudo-first and second-order models

In order to investigate the sorption process of TBBPA on adsorbent, pseudo-first-order model and pseudo-second-order model were used to check the validity. The kinetic models could be presented as followed:

$$\log(q_e - q_t) = \log q_e - \left(\frac{k_1}{2.303}\right)t \tag{2}$$

$$\frac{t}{q_t} = \frac{1}{k_2 q_e^2} + \left(\frac{1}{q_e}\right)t \tag{3}$$

where q_e was the maximum capacity, q_t was the amount of TBBPA adsorbed at time t, and k_1 and k_2 were the rate constants for pseudo-first-order model and pseudo-second-order model. The discrimination between pseudo-first-order model and pseudo-second-order model was performed by means of the statistical criteria described in the experimental section. Typical values for the model parameters and the statistical tests were shown in Tables 1 and 2. The figures of merit indicated the higher reliability of pseudo-second-order model. Fig. 1(a) also showed the typical curves in relation to the sets of data calculated from

the constants of pseudo-second-order model in Table 1. Therefore, adsorption of TBBPA onto K10 could be a pseudo-second-order process rather than pseudo-first-order process. The pseudo-second-order constants decreased from 16.41×10^{-2} to 2.75×10^{-2} for adsorption of TBBPA onto K10, when temperature was increased from 288 to 308 K. This implied that lower temperature favors the sorption process and increased the rate of approach to equilibrium in the TBBPA-K10 system.

3.2.2. Intra-particle diffusion model

Since pseudo-first and second-order models could not identify the sorption mechanism, the fit of intra-particle diffusion model was investigated.

$$q_t = k_i\, t^{0.5} + C \tag{4}$$

where k_i was the intra-particle diffusion rate constant and C was intercept for the intra-particle diffusion model. Results of this analysis on TBBPA data was illustrated in Fig. 1(b) as plots of q_t vs. $t^{0.5}$. The rate constant value (k_i) and intercept value C was listed in Table 1. According to this model, if the plot of uptake, q_t, vs. the square root of time, $t^{1/2}$ was linear and passed through the origin, then intra-particle diffusion is the only rate-controlling step. In Fig. 1(b), the plots were multi-linear, indicating multi-steps occurred. In theory, the first step was external surface sorption or instantaneous sorption stage, the second step was gradual sorption stage, where intra-particle diffusion was rate-controlled. The third step was the final equilibrium stage [26]. Fig. 1(b) showed that external surface sorption was apparent and completed in a few hours. Then, the stage of intra-particle diffusion attained. The third stage was absent over the whole range. It suggested that TBBPA slowly transported via intra-particle diffusion into the interlayer of K10 and finally retain in the interlayer. As a result, intra-particle diffusion played a significant role in the uptake of TBBPA by K10. In addition, the value of intra-particle

Table 1
The parameters of kinetics models for adsorption of TBBPA onto K10 montmorillonite at different temperature

Temperature (K)	Pseudo-first-order		Pseudo-second-order		Intra-particle diffusion		DEM				
	q_e	k_1	q_e	$k_2 \times 10^{-2}$	k_i	C	q_e	k_{D1}	k_{D2}	A_1	A_2
288	41.28	2.25	43.91	16.41	1.89	29.73	46.47	1.18	0.01	5.85	7.81
298	31.18	1.07	32.77	5.57	2.17	19.78	33.93	1.09	0.05	20.32	6.02
308	29.93	0.51	31.98	2.75	2.74	14.82	34.32	1.46	0.02	121.19	8.78

Table 2
Selected figures of merit for the pseudo-first-order, pseudo-second-order, and DEM models applied to the adsorption kinetics of TBBPA on K10

	Pseudo-first-order			Pseudo-second-order			DEM		
	288 K	298 K	308 K	288 K	298 K	308 K	288 K	298 K	308 K
t	2.42	3.61	1.97	2.01	4.33	2.08	0.37	2.98	1.23
SSE	4.28	61.15	39.40	287.42	4.42	23.42	5.24	1.43	6.63
R	0.82	0.83	0.94	0.95	0.99	0.98	0.99	0.99	0.99
R^2	0.68	0.69	0.88	0.91	0.99	0.97	0.99	0.99	0.98
PRESS	3.42	57.83	40.38	235.34	3.33	21.48	0.33	2.71	1.19
AIC	−6.72	−17.19	−12.71	−31.15	−6.43	−8.56	−5.97	−17.55	−4.07

diffusion rate constant was increased in the range of 288–308 K. When TBBPA diffused in the pore of adsorbent, the diffusion resistance decreased at higher temperature that caused the diffusion rate to increase [21].

3.2.3. Double-exponential model

When the adsorbent offered two different types of adsorption sites, such as the interlayer space and the external surfaces of the K10 montmorillonite, the double-exponential model (DEM), first proposed by Wilczak and Keinath [27], could be given as follow:

$$q_t = q_e - A_1 e^{-k_{D1}t} - A_2 e^{-k_{D2}t} \qquad (5)$$

where q_e and q_t were the adsorption capacities at equilibrium and at time t (min), respectively, and A_1 and A_2 were sorption rate parameters of the rapid and the slow step, respectively, and k_{D1} and k_{D2} were parameters controlling the mechanism. Typical values for the DEM parameters and the statistical tests were also shown in Tables 1 and 2. It was found that DEM fitted experimental data as well as pseudo-second-order model based on the model parameters and the statistical tests. Since pH in this section was in the range of 4.83–4.92, TBBPA only existed in neutral species. DEM equation could be applied to describe two-step sorption mechanism, which involved two steps, namely a rapid phase involving external and internal diffusions, followed by a slow phase controlled by the intra-particle diffusion [28]. In this case the two pre-exponential factor A_1 and A_2 in Eq. (5) corresponded to $\frac{D_1}{m_{ads}}$ and $\frac{D_2}{m_{ads}}$, where D_1 and D_2 were the diffusion parameters for the rapid and for the slow step, respectively, while m_{ads} was the adsorbent amount in the solution. According to this study, the value of D_1 increased with increasing temperature, suggesting that the rapid step involved external and internal diffusion and depended largely on the temperature. On the other hand, the slow step might be independent of the temperature. DEM could also describe a process where the adsorbent offered two different types of adsorption sites. On the first site, rapid TBBPA adsorption occurred where equilibration happened within a few minutes, whereas on the second site type, TBBPA adsorbed more slowly. Since the surface of K10 was heterogeneous it can be considered as a two site adsorbent. According to the results of models fitting, it could be observed that the best fits to the experimental data were obtained with the double-exponential and pseudo-second-order models for TBBPA.

3.3. Sorption and desorption isotherms

Adsorption isotherms indicated distribution of adsorbate between solution and adsorbent at the equilibrium state of the adsorption process [29]. The type of adsorption isotherm model was very important in order to understand the adsorption behavior for solid–liquid adsorption system. In this case, Langmuir, Freundlich, Langmuir–Freundlich (L–F), and Dubinin–Radushkevich (D–R) models were utilized to study the adsorption behavior of TBBPA. The pH in this section was in the range of 4.83–4.92.

3.3.1. Langmuir, Freundlich, and Langmuir–Freundlich isotherms

The Langmuir isotherm was based on the assumptions that adsorption took place at specific homogeneous sites within the adsorbent, there was no significant interaction among adsorbed species and the adsorbent was saturated after the formation of one layer of adsorbate on the surface of adsorbent. The Langmuir isotherm equation could be written as follow:

$$\frac{C_e}{q_e} = \frac{1 + K_L C_e}{K_L q_{max}} \tag{6}$$

where C_e was concentration of TBBPA at the equilibrium (mg/L); q_e was the amount of TBBPA adsorbed per mass unit of K10 at equilibrium (mg/kg); q_{max} was the amount of TBBPA adsorbed per mass unit of K10 at complete monolayer coverage (mg/kg); and K_L was Langmuir constant.

The Freundlich isotherm was an empirical equation employed to describe heterogeneous systems. The Freundlich equation was as follow:

$$q_e = K_f C_e^n \tag{7}$$

where C_e was concentration of TBBPA at the equilibrium (mg/L); q_e was the amount of TBBPA adsorbed per mass unit of K10 at equilibrium (mg/kg); K_f and n were the Freundlich adsorption isotherm constants, being indicative of the extent of the adsorption and the degree of nonlinearity between solution concentration and adsorption, respectively.

Langmuir–Freundlich (L–F) model was given as follow:

$$\frac{C_e^n}{q_e} = \frac{1 + K_{LF} \, C_e^n}{K_{LF} \, q_{max}} \tag{8}$$

where C_e was concentration of TBBPA at the equilibrium (mg/L); q_e was the amount of TBBPA adsorbed per mass unit of K10 at equilibrium (mg/kg); q_{max} was the amount of TBBPA adsorbed per mass unit of K10 (mg/kg); and K_{LF} and n was model constants for L–F model. The parameters obtained from Langmuir, Freundlich, and L–F models were listed in Table 3.

Fig. 2 showed the sorption and desorption isotherms at three different temperatures. None of the isotherms data exhibited an apparent adsorbent saturation, which implied a good maximum sorption capacity for removal of TBBPA by K10. Analogously to the procedure applied for the analysis of the kinetic data, the discrimination among the different models had been performed by means of the statistical criteria shown in Table 4. All the statistical tests suggested that the models which gave the better fit to experimental data were Freundlich model and L–F model.

The Freundlich constant K_f was considered as the relative indicator of sorption capacity. The calculated K_f obtained from sorption isotherms was 2.06×10^3, 0.62×10^3, and 0.63×10^3 for 288, 298, and 308 K, respectively. The calculated K_f obtained from desorption isotherms was 2.41×10^3, 0.81×10^3, and 1.09×10^3, respectively. It was observed that highest value was obtained at 288 K, which indicated the sorption capacity and intensity from 288 to 308 K was enhanced at lower temperature. This result was in good agreement with the results found in adsorption of promethazine hydrochloride onto K10 [21]. The exponent n was an index of the diversity of free energies associated with the sorption of the solute by multiple components of the heterogeneous sorbent. In the present case, n was larger than one and increased with the temperature increasing which meant that the temperature slightly enhanced the free energies and hampered further adsorption. Therefore, it could be concluded that adsorption rather than partition was responsible for the overall process.

The L–F model produced the best fit for the adsorption of TBBPA on K10, supported by the highest correlation coefficients and lowest value of PRESS and AIC. The L–F model was a compromise between the Langmuir and Freundlich model and incorporated

Table 3
Parameters of Langmuir, Freundlich, and D–R equations for sorption and desorption of TBBPA on K10 at different temperatures

Model		Sorption			Desorption		
		288 K	298 K	308 K	288 K	298 K	308 K
Langmuir	$q_{max} \times 10^9$	15.91	14.13	20.78	3.06	0.02	17.69
	$K_L \times 10^{-8}$	5.56	2.23	1.51	72.67	2.75	3.66
Freundlich	$K_f \times 10^3$	2.06	0.62	0.63	2.41	0.81	1.09
	n	1.38	1.47	1.62	1.02	1.01	1.26
L–F	q_{max}	227.27	99.01	200.01	238.41	188.67	666.67
	K_{LF}	44.01	12.63	25.21	53.78	26.53	15.01
	n	1.81	1.56	2.69	1.42	1.55	2.08
D–R	q_{max}	418.57	150.12	397.68	513.71	276.16	509.79
	$\beta \times 10^{-8}$	4.64	1.35	11.51	3.33	4.11	7.13
	E	3.28	6.08	2.08	4.08	3.49	2.65
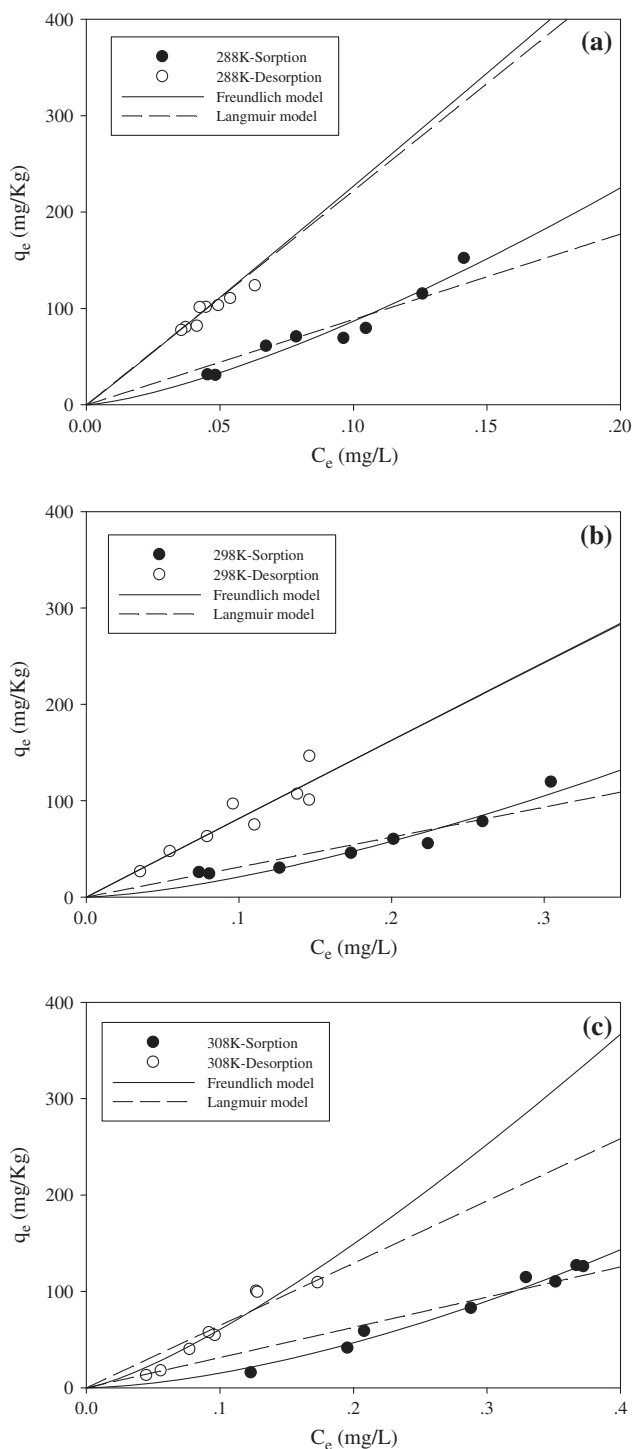
Fig. 2. Isotherms for sorption and desorption of TBBPA onto K10 at 288 K (a), 298 K (b), and 308 K (c), respectively (K10—0.1 g; pH 4.83–4.92; the solid line represent sorption isotherms fitted by Freundlich model; the dotted lines represent sorption isotherms fitted by Langmuir model).

the advantages of both Langmuir and Freundlich equation. This model could be applied either to homogeneous or heterogeneous surface. Thus, sorption of TBBPA on K10 might occur on both homogeneous and heterogeneous sorbent surfaces.

3.3.2. Dubinin–Radushkevich isotherms

In order to determine the adsorption type, D–R isotherm model was applied to adsorption data:

$$\ln q_e = \ln q_{max} - \beta \varepsilon^2 \qquad (9)$$

$$\varepsilon = RT \ln\left(1 + \frac{1}{C_e}\right) \qquad (10)$$

where q_e (mg/kg) is the amount of adsorbed TBBPA per unit mass of sorbent, q_{max} (mg/kg) is the theoretical saturation capacity, C_e (mg/L) is the concentration of TBBPA at the equilibrium, β is a constant related to the adsorption energy, and T is temperature (K). R is the gas constant (KJ/mol K). The D–R parameters were listed in Table 3. According to the Eqs. (9) and (10), the sorption free energy could be further obtained as follow:

$$E = -(2\beta)^{-1/2} \qquad (11)$$

The magnitude of E was useful for estimating the type of adsorption process. If the E value was smaller than 4.2 KJ/mol, adsorption type considered as physical sorption. If the E value was bigger than 16 KJ/mol, adsorption type was regarded as the chemical sorption. The values of E as listed in Table 3 were found from 2.08 to 6.08 KJ/mol. In most case, the value of E was lower than 4.2 KJ/mol, which indicated physical adsorption.

3.3.3. Desorption hysteresis

As shown in Table 4, the Freundlich model fitted desorption isotherm well. The apparent sorption–desorption hysteresis was quantified for sorbent–solute–solution system using HI [8]:

$$HI = \frac{q_e^d - q_e^s}{q_e^s}\bigg|T, C_e \qquad (12)$$

where q_e^s and q_e^d were the amounts of TBBPA adsorbed for the single-cycle sorption and desorption

Table 4
Selected figures of merit for the Langmuir, Freundlich, and Langmuir–Freundlich (L–F) models applied to the adsorption isotherms of TBBPA on K10

Model		Sorption			Desorption		
		288 K	298 K	308 K	288 K	298 K	308 K
Langmuir	T	1.41	13.90	1.34	2.40	19.26	1.46
	SSE	1.4×10^3	13.8×10^3	56.1×10^3	61.6×10^3	64.3×10^3	32.5×10^3
	R	0.96	0.96	0.97	0.88	0.95	0.97
	R^2	0.93	0.93	0.94	0.78	0.91	0.94
	PRESS	0.6×10^3	0.5×10^3	27.1×10^3	0.2×10^3	2.2×10^3	12.5×10^3
	AIC	−41.47	−59.66	−70.83	−71.59	−71.93	−66.48
Freundlich	T	0.39	0.19	0.51	3.20	0.48	0.91
	SSE	0.7×10^3	2.7×10^3	0.3×10^3	0.9×10^3	1.7×10^3	1.1×10^3
	R	0.99	0.99	0.99	0.95	0.97	0.98
	R^2	0.98	0.98	0.99	0.91	0.94	0.96
	PRESS	1.3×10^3	0.3×10^3	0.6×10^3	0.3×10^3	2.7×10^3	6.9×10^3
	AIC	−34.06	−44.90	−26.51	−36.28	−41.23	−37.03
L–F	T	0.24	0.96	1.49	0.80	1.46	5.45
	SSE	1.3×10^3	0.1×10^3	0.3×10^3	0.2×10^3	1.9×10^3	2.2×10^3
	R	0.99	0.99	0.99	0.98	0.99	0.99
	R^2	0.98	0.98	0.99	0.97	0.99	0.99
	PRESS	27.2×10^3	0.2×10^3	0.6×10^3	0.2×10^3	1.8×10^3	2.8×10^3
	AIC	−38.73	−19.05	−27.26	−23.28	−41.91	−52.14

experiments, respectively. The subscript T and C_e specify conditions of constant temperature and residual solution phase concentration. In previous study, a negative or zero value of HI indicated that sorption–desorption hysteresis insignificant [8]. The values of HI at three temperatures and three equilibrium concentrations ($C_e = 0.05$, 0.10, and 0.50 mg/L) were calculated through Freundlich model parameters and the results was shown in Fig. 3. All of the HI values were above zero, which implied occurrence of sorption–desorption Hysteresis of TBBPA. It may be attributed to the distribution into interlayer and some irreversible binding to some specific adsorption site. Additionally, the HI value increased with increase in temperature, which indicated that high temperature enhanced the sorption–desorption hysteresis.

3.4. Effects of pH

The pH value of solution was an important controlling parameter in the sorption process. The obtained result in Fig. 4 showed the change in the amounts of adsorbed TBBPA by K10 with the pH ranging from 3.0 to 9.0. It was observed that uptake of TBBPA by K10 tended to decrease significantly when pH increased from 5.5 to 8.0. This result was consistent with the uptakes of TBBPA by soils, carbon nanotubes, and graphene oxide [8–10,23].
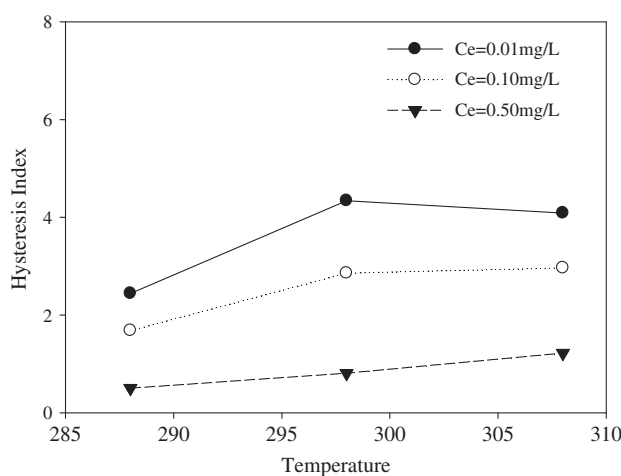
Fig. 3. HI calculated from Freundlich isotherms model at three temperature (288, 298, and 308 K) and three equilibrium concentrations ($C_e = 0.01$, 0.10, and 0.50 mg/L).

The Si–O group on the external surface of clays could be further convert to Si–OH group at different pH environment employed. At alkaline condition, the surface group was fully or partially deprotonated and increased the negative charge on the surface of clays. The negative charge on the surface of clays was not available for adsorption of anion molecular. Therefore, the uptakes of some anion pollutants were reduced at
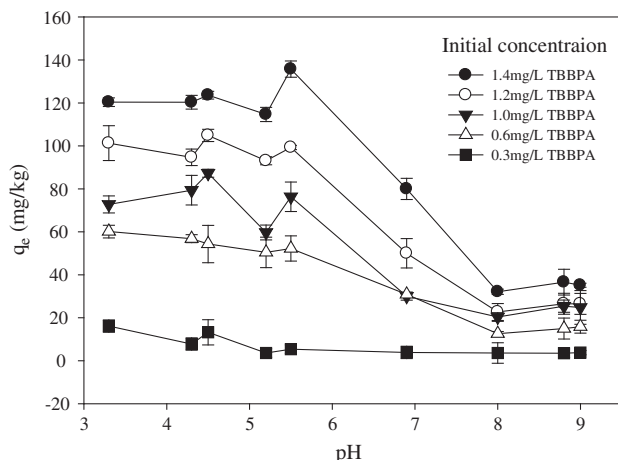
Fig. 4. Effects of pH on adsorption of TBBPA onto K10 (TBBPA—(0.3–1.4 mg/L); T—298 K).

alkaline condition. Moreover, TBBPA has two proton-binding sites, carboxyl and piperazinyl with pK_a values of 7.5 and 8.5 [8]. At pH > 7.5, TBBPA was mainly in the form of negatively charged phenoxy ion and the electrostatic repulsion between the TBBPA and negative charged surface of K10 led to decrease in sorption capacity. At strongly acidic pH, TBBPA was predominantly in the neutral molecular form. The electrostatic repulsion became weak. As a result, the acidic condition was available for adsorption of TBBPA onto K10 montmorillonite. The equilibrium amounts of TBBPA adsorbed onto K10 at five initial concentrations were used to construct adsorption isotherm and the Freundlich isotherm model parameters (K_f and n) obtained from three pH condition (3.3, 7.8, and 9.7) was collected in Table 5. It was observed that the K_f value at pH 3.3 was larger than those at pH 7.8 and 9.7, which meant acidic condition was favorable for the adsorption of TBBPA onto K10. The Freundlich exponent n was about 1 at pH 3.3, which indicated that the adsorption sites are almost homogeneous in energy, while the n value less than one obtained at pH 7.8 and 9.0 implied that alkaline condition modified the sorbent in a manner that decreased the sorption capacity, such as deprotonated parts of adsorption sites.

Table 5
Parameters for Freundlich model obtained from different pH condition

	pH 3.3	pH 7.8	pH 9.0
K_f	673.23	18.87	23.94
n	1.12	0.78	0.68

3.5. Effects of ions strength

A variety of major ions, including nitrate (NO_3^-), sulfate (SO_4^{2-}), phosphate (HPO_4^{2-} and PO_4^{3-}), carbonate (HCO_3^-), sodium (Na^+), potassium (K^+), calcium (Ca^{2+}), zinc (Zn^{2+}), or nickel (Ni^{2+}), were investigated to figure out the effects of ions on TBBPA uptake by K10. The initial concentration of TBBPA was 1.0 mg/L in all experiments, whereas concentrations of ions were 1.0, 5.0, and 10.0 mg/L respectively. As shown in Fig. 5, some anions exhibited obvious negative effect on removal efficiency. Moreover, the presence of PO_4^{3-} and NO_3^{2-} significantly decreased sorption capacity, while HCO_3^-, HPO_4^{2-}, and SO_4^{2-} did not disturb the amount of TBBPA uptake by K10. Fig. 5 also showed that the TBBPA uptake was increased by the presence of cations in solution. In most case, the removal efficiency was increased with increasing initial concentration of cations. It was probably due to that cations could format neutral ion pairs and screen the negative charge of clay surface. Previous study demonstrated that TBBPA sorption in soils was significantly influenced by Ca^{2+} [8]. In this work, adsorption of TBBPA onto K10 was influenced by all of the selected cations, and the ability of major cations with 10 mg/L initial concentration increased sorption capacity in this order of $Ni^{2+} > K^+ > Zn^{2+} > Ca^{2+} > Na^+$. K10 in the presence of Ni^{2+} exhibited the best sorption capacity because Ni^{2+} was the transition metal, which was known to undergo complexation with aromatic groups of TBBPA based on an electron donation and back donation process. There had been observed during studies related to the interaction of transition metals and drugs which showed excellent ability of removing contaminants from aqueous solution [30]. In
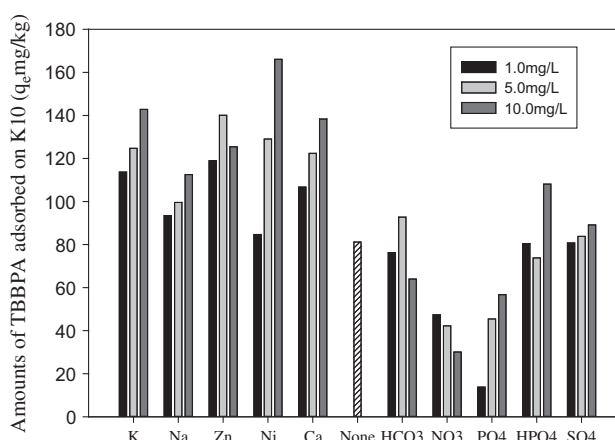
Fig. 5. Effects of ions strength for adsorption of TBBPA on K10 (TBBPA—1.0 mg/L; T—298 K, initial concentration of ions was 1.0, 5.0, and 10.0 mg/L, respectively).

conclusion, cations significantly improved the sorption capacities of K10 montmorillonite for removing TBBPA from aqueous solution, while parts of anions depressed the sorption process.

3.6. Effects of surfactants

Surfactants were regarded as effective materials to modify clays through ions exchange. The effects of surfactants were conducted by varying surfactants concentrations and the result was shown in Fig. 6. Surfactants were firstly added into the K10–water system for 12 h, and then followed by the injection of TBBPA stock solution into the system. The initial concentration of TBBPA was 1.0 mg/L, whereas TBBPA uptakes increased from 80 to 180 mg/kg when CTMAB concentration varied from 2 to 80 mg/L. However, uptake of TBBPA in coexisting SDS in solution was decreased. When both SDS and CTMAB were added into the solution, TBBPA uptakes significantly increased with increasing surfactants. This indicated that CTMAB had an important influence on adsorption of TBBPA onto K10. In previous studies, CTMAB had been utilized to modify clays in order to enhance adsorption of different organic contaminants [31]. The permanent negative charge within the crystal structures of clay minerals make them suitable for surface modification by long chain or short chain organic cation surfactants. The modified clays provide primarily a hydrophobic environment towards TBBPA, resulting in a further higher sorption. In this work, it was probable that TBBPA and CMTAB entered into the K10 montmorillonite and formed processes including synthesis of organic modified clays and removal of TBBPA from water.

3.7. FTIR analysis

The FTIR spectrum of TBBPA, K10, and K10-loaded TBBPA was shown in Fig. 7. The intense band at 3,620 cm^{-1} was assigned to internal O–H groups of K10. The stretching vibration of water was observed at 3,440 cm^{-1} in Fig. 7. Compared to K10, it was seen that the band for stretching vibration of water was shifted to 3,432 cm^{-1} after TBBPA adsorption. According to the previous study of Bekçi et al. [20], the shift of stretching vibration of water was related to hydrogen bonding. This indicated that hydrogen bonding might occur between water molecules and TBBPA. In spectrum of K10, the band at 1,635 cm^{-1} was assigned to water deformation vibration. Intensive band at 1,048 cm^{-1} can be attributed to Si–O stretching vibrations. The Si–O–Al and Si–O–Si bending vibrations appear at 521 and 468 cm^{-1}, respectively. No more differences between K10 and K10-loaded TBBPA were observed in FTIR spectrum, indicating the main sorption mechanism was physical sorption rather than ion exchange reaction.

In order to figure out if organoclays had been formed in the surface or interlayer of K10, two stages were investigated for adsorption of TBBPA in the presence of CTMAB. In the first stage, CTMAB was added into the K10–water system for 12 h. In the second stage, adsorption of TBBPA on organoclays was performed. A comparison of the FTIR spectrum between K10-loaded CTMAB and K10-loaded CTMAB+TBBPA was also shown in Fig. 7. In the first stage, the characteristic adsorption bands at around 2,969 and 2,853 cm^{-1} was attributed to symmetric and asymmetric stretching vibration of the –CH$_2$ and –CH$_3$, suggesting that CTMAB was successfully

Fig. 6. Effects of coexisting surfactants on TBBPA adsorption onto K10 (TBBPA—1.0 mg/L; T—298 K).
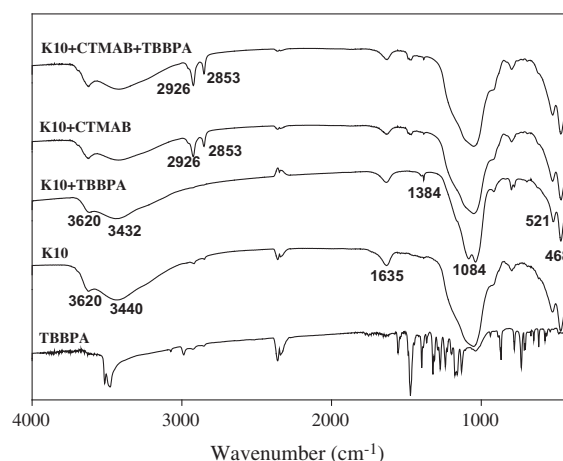
Fig. 7. FTIR spectrum of TBBPA, K10, K10-loaded TBBPA, K10-loaded CTMAB and K10-loaded CTMAB + TBBPA.

Table 6
The thermodynamics parameters for the sorption of TBBPA on K10

Absorbent	Temperature (K)	ΔG (KJ/mol)	ΔH (KJ/mol)	ΔS (J/K mol)
K10 montmorillonite	288	−16.28	–	–
	298	−14.45	−46.56	−0.11
	308	−14.27	–	–

intercalated into the surface or interlayers of clays. The FTIR spectrum in the second stage was similar to that in the first stage. Bands at 2,969 and 2,853 cm^{-1} were observed in adsorption of TBBPA in the presence of CTMAB. This indicated adsorption of TBBPA on K10 was greatly enhanced by the CTMAB intercalation probably due to hydrophobic interaction.

3.8. Thermodynamics

The thermodynamic parameters, such as free energy (ΔG), enthalpy change (ΔH), and entropy change (ΔS), were calculated to find the feasibility and exothermic nature, based on the methods defined by Fasfous et al. [25].

The constant K_0 could be defined as:

$$K_0 = \frac{\alpha_q}{\alpha_C} = \frac{\gamma q_e}{\gamma C_e} = \frac{q_e}{C_e} \qquad (13)$$

where α_q was the activity of TBBPA adsorbed on K10, α_c was the activity of TBBPA in solution at equilibrium, and γ was the activity coefficient. Since the concentration of TBBPA in solution approaches zero, the activity coefficient approached unity. The value of K_0 was confirmed through plotting the ln K_0 vs. q_e, and exploring the q_e to zero. The straight line obtained was fitted using linear least-squares analysis methods. The intercept of vertical axis was regarded as ln K_0.

The values of free energy (ΔG), enthalpy change (ΔH), and entropy change (ΔS) were calculated by the equation as follow:

$$\Delta G = -RT \ln K_0 \qquad (14)$$

$$\ln K_0 = -\frac{\Delta H}{RT} + \frac{\Delta S}{R} \qquad (15)$$

where R was universal gas constant (8.314 J/mol K) and T was the sorption temperature in Kelvin. The value of ΔG was calculated from Eq. (14). The value of ΔH and ΔS was confirmed by the slope and intercept of Eq. (15). All of the results were presented in Table 6. The results showed that the change in the free energy (ΔG) with negative values for −16.28, −14.45, and −14.27 KJ/mol at all experiment temperature indicated

that adsorption of TBBPA on K10 was spontaneous and that the system did not gain energy from an external source. When temperature decreased from 308 to 288 K, the magnitude of ΔG value shifted to high negative value (from −14.27 to −16.28 KJ/mol) suggested that the adsorption was more spontaneous at low temperature. Since the value of enthalpy change (ΔH) was −46.56 KJ/mol, interaction of TBBPA molecule with K10 was exothermic by nature. Moreover, the value of enthalpy change was slightly higher than the value of 40 KJ/mol, which indicated that the main sorption process was physical sorption. The negative entropy change (ΔS) value corresponded to a decrease in the degree of freedom of the adsorbed species. The small entropy showed that K10 structure did not change significantly as a result of adsorption.

4. Conclusions

This study investigated the adsorption of TBBPA onto K10 montmorillonite. The results of kinetic experiment showed that the sorption was pseudo-second-order and sorption may be controlled by the intra-particle diffusion. DEM model also fitted that experimental data well based on the statistical test. The nonlinear sorption isotherms and desorption hysteresis were observed and Freundlich model and Langmuir–Freundlich model describe the sorption behavior of TBBPA well. The negative values of ΔG and ΔH indicated exothermic nature and spontaneity, respectively. The negative entropy change (ΔS) value corresponded to a decrease in the degree of freedom of the adsorbed species. It was observed from experiment of pH that sorption capacity depended on pH and maximum sorption capacity can be reached at acidic condition. Additionally, metal cations and cationic surfactants had positive effects on adsorption of TBBPA onto K10. The results of present study showed that K10 could be regarded as a potential adsorbent for removal of TBBPA from aqueous solution.

Acknowledgments

Technology and National Key Scientific and Technological Project ''Water Pollution Control and Treatment'' (2012ZX07206002 and 2012ZX07206004).

References

[1] U. Sellström, B. Jansson, Analysis of tetrabromobisphenol A in a product and environmental samples, Chemosphere 31(4) (1995) 3085–3092.
[2] A. Covaci, S. Voorspoels, M.A.E. Abdallah, T. Geens, S. Harrad, R.J. Law, Analytical and environmental aspects of the flame retardant tetrabromobisphenol-A and its derivatives, J. Chromatogr. A 1216(3) (2009) 346–363.
[3] H. Takigami, G. Suzuki, Y. Hirai, S. Sakai, Brominated flame retardants and other polyhalogenated compounds in indoor air and dust from two houses in Japan, Chemosphere 76(2) (2009) 270–277.
[4] C. Sánchez-Brunete, E. Miguel, J.L. Tadeo, Determination of tetrabromobisphenol-A, tetrachlorobisphenol-A and bisphenol-A in soil by ultrasonic assisted extraction and gas chromatography–mass spectrometry, J. Chromatogr. A 1216(29) (2009) 5497–5503.
[5] X. Peng, Z. Zhang, Z. Zhao, X. Jia, 16S ribosomal DNA clone libraries to reveal bacterial diversity in anaerobic reactor-degraded tetrabromobisphenol A, Bioresour. Technol. 112 (2012) 75–82.
[6] X. Peng, Z. Zhang, W. Luo, X. Jia, Biodegradation of tetrabromobisphenol A by a novel Comamonas sp. strain, JXS-2-02, isolated from anaerobic sludge, Bioresour. Technol. 128 (2013) 173–179.
[7] X. Peng, X. Jia, Optimization of parameters for anaerobic co-metabolic degradation of TBBPA, Bioresour. Technol. 148 (2013) 386–393.
[8] Z. Sun, Y. Yu, L. Mao, Z. Feng, H. Yu, Sorption behavior of tetrabromobisphenol A in two soils with different characteristics, J. Hazard. Mater. 160(2–3) (2008) 456–461.
[9] Y. Zhang, Y. Tang, S. Li, S Yu Sorption and removal of tetrabromobisphenol A from solution by graphene oxide, Chem. Eng. J. 222 (2013) 94–100.
[10] W. Han, L. Luo, S. Zhang, Adsorption of tetrabromobisphenol A on soils: Contribution of soil components and influence of soil properties, Colloids Surf., A 428 (2013) 60–64.
[11] Bromine Science and Environmental Forum, 2000. Available from: <http://www.bsef.com/>.
[12] C.A. de Wit, An overview of brominated flame retardants in the environment, Chemosphere 46(5) (2002) 583–624.
[13] M. Alaee, P. Arias, A. Sjödin, Å Bergman, An overview of commercially used brominated flame retardants, their applications, their use patterns in different countries/regions and possible modes of release, Environ. Int. 29(6) (2003) 683–689.
[14] I. Watanabe, S. Sakai, Environmental release and behavior of brominated flame retardants, Environ. Int. 29(6) (2003) 665–682.
[15] R. H. Boecker, B. Schwind, V. Kraus, S. Pullen, G. Tiegs, Cellular disturbances by various brominated flame retardants, Second International Workshop on Brominated Flame Retardants 2001, pp. 14–16.
[16] S. Pullen, R. Boecker, G. Tiegs, The flame retardants tetrabromobisphenol A and tetrabromobisphenol A-bisallylether suppress the induction of interleukin-2 receptor α chain (CD25) in murine splenocytes, Toxicology 184(1) (2003) 11–22.
[17] Y.-F. Zhang, W. Xu, Q.-Q. Lou, Y.-Y. Li, Y.-X. Zhao, W.-J. Wei, Z.-F. Qin, H.-L. Wang, J.-Z. Li, Tetrabromobisphenol A disrupts vertebrate development via thyroid hormone signaling pathway in a developmental stage-dependent manner, Environ. Sci. Technol. 48(14) (2014) 8227–8234.
[18] L. Canesi, L.C. Lorusso, C. Ciacci, M. Betti, G. Gallo, Effects of the brominated flame retardant tetrabromobisphenol-A (TBBPA) on cell signaling and function of Mytilus hemocytes: Involvement of MAP kinases and protein kinase C, Aquat. Toxicol. 75(3) (2005) 277–287.
[19] H. Zaghouane-Boudiaf, M. Boutahala, Adsorption of 2, 4, 5-trichlorophenol by organo-montmorillonites from aqueous solutions: Kinetics and equilibrium studies, Chem. Eng. J. 170(1) (2011) 120–126.
[20] Z. Bekçi, Y. Seki, M. Kadir Yurdakoç, A study of equilibrium and FTIR, SEM/EDS analysis of trimethoprim adsorption onto K10, J. Mol. Struct. 827(1–3) (2007) 67–74.
[21] G. Gereli, Y. Seki, İ. Murat Kuşoğlu, K. Yurdakoç, Equilibrium and kinetics for the sorption of promethazine hydrochloride onto K10 montmorillonite, J. Colloid Interface Sci. 299(1) (2006) 155–162.
[22] W. Huang, H. Yu, W.J. Weber Jr., Hysteresis in the sorption and desorption of hydrophobic organic contaminants by soils and sediments, J. Contam. Hydrol. 31(1–2) (1998) 129–148.
[23] R. Todeschini, Introduzione alla Chemiometria (Introduction to Chemometrics), Edises, Napoli, 1998, p. 321.
[24] T.P. Ryan, Modern Regression Methods, Wiley, New York, NY, 1997.
[25] I.I. Fasfous, E.S. Radwan, J.N. Dawoud, Kinetics, equilibrium and thermodynamics of the sorption of tetrabromobisphenol A on multiwalled carbon nanotubes, Appl. Surf. Sci. 256(23) (2010) 7246–7252.
[26] Y. Shu, L. Li, Q. Zhang, H. Wu, Equilibrium, kinetics and thermodynamic studies for sorption of chlorobenzenes on CTMAB modified bentonite and kaolinite, J. Hazard. Mater. 173(1–3) (2010) 47–53.
[27] A. Wilczak, T.M. Keinath, Kinetics of sorption and desorption of copper(II) and lead(II) on activated carbon, Water Environ. Res. 65 (1993) 238–244.
[28] I. Calabrese, G. Cavallaro, C. Scialabba, M. Licciardi, M. Merli, L. Sciascia, M.L. Turco Liveri, Montmorillonite nanodevices for the colon metronidazole delivery, Int. J. Pharm. 457(1) (2013) 224–236.
[29] M.K. Seliem, S. Komarneni, T. Byrne, F.S. Cannon, M.G. Shahien, A.A. Khalil, I. Abd El-Gaid, Removal of nitrate by synthetic organosilicas and organoclay: Kinetic and isotherm studies, Sep. Purif. Technol. 110 (2013) 181–187.
[30] W.A. Cabrera-Lafaurie, F.R. Román, A.J. Hernández-Maldonado, Transition metal modified and partially calcined inorganic–organic pillared clays for the adsorption of salicylic acid, clofibric acid, carbamazepine, and caffeine from water, J. Colloid Interface Sci. 386(1) (2012) 381–391.
[31] S.M. Lee, D. Tiwari, Organo and inorgano-organo-modified clays in the remediation of aqueous solutions: An overview, Appl. Clay Sci. 59–60 (2012) 84–102.